Macromolecules

Article

pubs.acs.org/Macromolecules

Shape-Memory Polymers with Adjustable High Glass Transition Temperatures

Xinli Xiao,[†,‡] Deyan Kong,[‡] Xueying Qiu,[‡] Wenbo Zhang,[‡] Fenghua Zhang,[†] Liwu Liu,[§] Yanju Liu,[§] Shen Zhang,[‡] Yang Hu,[‡] and Jinsong Leng*[,†]

[†]Centre for Composite Materials and Structures, Harbin Institute of Technology, No. 2 YiKuang Street, Harbin 150080, People's Republic of China

[‡]Department of Chemistry and [§]Department of Astronautical Science and Mechanics, Harbin Institute of Technology, No. 92 West Dazhi Street, Harbin 150001, People's Republic of China

Supporting Information

ABSTRACT: Shape-memory polymers (SMPs) are synthesized with adjustable glass transition temperature (T_g) ranging from 299 to 322 °C, higher than those reported previously. The polyimide containing thermal stable but flexible linkages within the backbone act as reversible phase, and high molecular weight (M_n) is necessary to form physical cross-links as fixed phase of thermoplastic shape-memory polyimide. The critical M_n is 21.3 kg/mol, and the relationship between M_n and T_g is explored. Thermoset polyimides show higher storage modulus and better shape-memory effects than thermoplastic counterparts due to covalent cross-linking, and the effective cross-link density with the influence on their physical properties is studied. The mechanism of high-temperature shape-memory effect of polyimide on the basis of chain flexibility, molecular weight, and cross-link density is proposed, which will benefit further research on high-temperature SMPs.

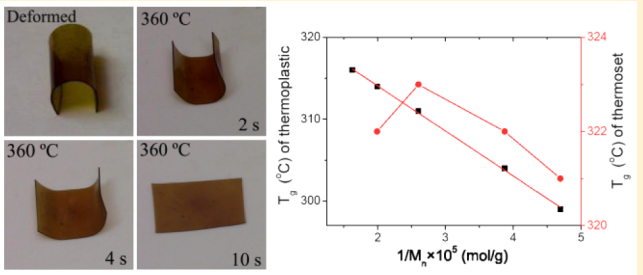

INTRODUCTION

Shape-memory polymers (SMPs) have attracted much attention from various fields that require light weight and large recoverable strains.[1−8] Thermal energy is the main stimulus for shape recovery process, although other stimuli such as light, solvent, and electrical and magnetic fields are reported.[9−17] The bulk of the research to date has concentrated on SMPs with relatively low to medium shape transition temperature for applications in biomedical and surgical materials, smart fabrics, temperatures sensors, actuators, and so on.[18−22]

High-temperature SMPs have wide potential applications in severe conditions that undergo high temperatures, such as deployable space structures, shape morphing structures, smart jet propulsion system, and high-temperature sensors and actuators.[5,23−25] The glass transition temperature (T_g) is usually taken as the shape transition temperature for high temperature SMPs, and T_g of the SMP should be higher than the environmental temperatures to ensure that shape recovery process will not be prematurely triggered by the environment.[7,26] Therefore, SMPs with different controllable T_g are required to fulfill the demands of different environments. There have been several reports about high temperature SMPs in recent years, such as thermoset polyaspartimide, thermoplastic and thermoset polyimide, and thermoset cyanate.[26−31] The reported highest T_g of 288 °C was observed in thermoplastic shape-memory sulfonated poly(ether ether ketone) ionomers, but the maximum temperature for processing and shape-memory design was limited by the desulfonation of the ionomers, which occurred above 300 °C.[31]

Aromatic polyimide (PI) possesses excellent properties such as high T_g, high thermal stability, high tensile strength, and excellent radiation shielding capability, which make them attractive materials for aerospace, electronics, and automobiles.[32−36] Besides the common applications as adhesive coating and film-forming materials, PIs have also been used as flexible cables, bushings, bearings, socket, or constructive parts.[37,38] Therefore, shape-memory polyimide that combines the shape-memory effects with the unusual properties of PI is expected to extend applications in many fields. Here we present a series of shape-memory polyimides possessing adjustable T_g over 300 °C, high thermal stability, and excellent shape-memory properties.

The shape-memory polyimides here are obtained by polycondensation of 4,4′-(hexafluoroisopropylidene)diphthalic anhydride (6FDA) and 4,4′-diaminodiphenyl ether (ODA), and the hexafluoroisopropylidene and ether linkages within the backbone make the polyimide chains suitable for the reversible phase of shape-memory process. The relative flexibility mainly accounts for the T_g higher than those of the previously reported

Received: March 29, 2015
Revised: May 12, 2015

DOI: 10.1021/acs.macromol.5b00654
Macromolecules XXXX, XXX, XXX−XXX

SMPs. Molecular weight has been observed to exert influence on the physical properties of many polymers,[39,40] and number-average molecular weight (M_n) was reported to affect the shape-memory behavior and thermomechanical properties of thermoplastic SMPs such as polyurethanes (SMPUs).[41] Polyimide samples with different M_n are obtained, and high M_n is demanded to form physical cross-links as the permanent phase of thermoplastic shape-memory polyimide. The critical M_n that exhibits shape-memory effect is obtained, and the relationships between M_n and the physical properties of thermoplastic shape-memory polyimide are explored.

Thermoset SMPs are preferred in many cases as they are intrinsically chemical resistant and possess higher storage modulus and better shape-memory performances than thermoplastic SMPs due to the covalent cross-links.[42,43] Here thermoset shape-memory polyimide samples are fabricated by employing tris(4-aminophenyl)amine (TAP) as cross-linkers, and the influence of covalent cross-linking on the physical properties, such as storage modulus, T_g, and shape-memory performances, is investigated.

By analyzing the relationships between chemical structures and physical properties, the possible mechanism of high-temperature shape-memory effect of polyimide based on chain flexibility, molecular weight, and cross-link density is proposed.

EXPERIMENTAL METHODS

Synthesis of Thermoplastic Polyimide. 6FDA (99%) and ODA (98%) were purchased from Sigma-Aldrich Co. TAP (98%) was purchased from TCI Chemicals, and the chemicals were used as received. Dimethylacetamide (DMAc) was purchased from Kemiou Chemical Reagent Co. Ltd. and distilled with activated 4 Å molecular sieves under reduced pressure. All the lab instruments and glassware for the synthesis must be strictly dry. The shape-memory polyimide was synthesized by polycondensation of 6FDA and ODA, and the schematic illustration for the process is shown in Figure 1.

ODA and 20 mL of DMAc were added to a three-necked flask and then stirred under dry nitrogen for 25 min. 4 mmol of 6FDA was fed into the flask in batches within 1 h, and intense mechanical stirring was executed at room temperature for 20 h to form highly viscous PAA. The flask was transferred into a vacuum drying chamber and heated under vacuum at 50 °C for 3 h to remove the bubbles. In order to obtain the polyimide sheet with rather uniform thickness, an air-bubble level was employed to characterize the horizontal plane of the heater platform, and small thin sheet irons are used as backup plates to make sure that the glass substrate is horizontal. The PAA was poured on the glass plate and underwent a stepwise imidization curing process at 80 °C/2 h, 120 °C/2 h, 170 °C/2 h, 200 °C/2 h, 260 °C/1 h, 300 °C/1 h, and 330 °C/1 h. The polyimide samples were detached away from glass in deionized water and was heated at 180 °C for 3 h to remove the water. Polyimide with different M_n values were prepared by varying the molar ratio of 6FDA to ODA.

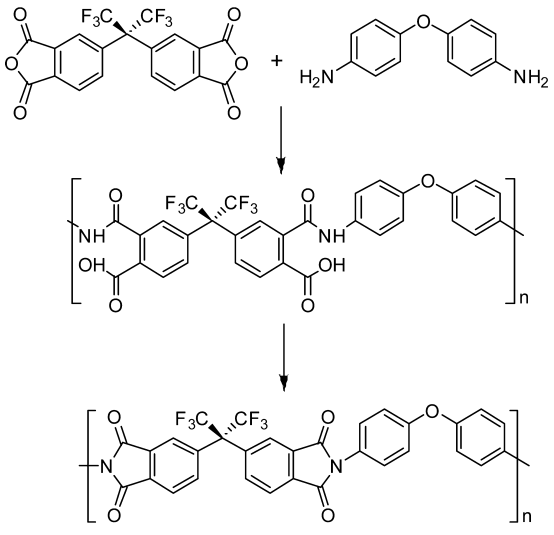

Figure 1. Schematic of polycondensation of thermoplastic polyimide. 6FDA and ODA formed viscous poly(amic acid) (PAA), and PAA transformed into polyimide by thermal curing.

Synthesis of Thermoset Polyimide. The highly viscous PAAs were obtained with the same procedures, and TAP was then added to the PAA solution, where the total amount of amine groups (2 in one ODA molecule and 3 in one TAP molecule) was equal to that of anhydride group (2 in one 6FDA molecule). The mixture was stirred for another 6 h and then underwent the vacuum evaporation and thermal imidization as mentioned above.

Molecular Weight and Structure Characterization. The molecular weights of the polyimide samples were determined by size exculsion chromotography (SEC) using a Waters 2414 equipped with a refractive index detector in a mixture of *N*-methyl-2-pyrrolidone (NMP) and 0.05 M lithium bromide at 60 °C, and the molecular weight versus evolution time was calculated using narrow polydispersity poly(styrene) standards. The structure of the shape-memory polyimide is studied by Fourier transform infrared spectroscopy (FTIR) on Thermo Nicolet Nexus 870.

Thermomechanical Characterization. The storage modulus and loss factor of the specimens versus temperature are characterized by dynamic mechanical analysis (DMA) on Netzsch Q800. DMA tests were conducted in tensile mode at the frequency of 1 Hz with a heating rate of 3 °C/min on slabs with the dimension of 36 mm × 3 mm × 0.12 mm. The thickness of the slabs was the thickness of the film, and only the samples with uniform thickness are chosen for DMA analysis. Three tests were conducted for per material with each exhibiting the consistent results, and only one DMA spectra is shown for clarity.

Thermal Measurement. Differential scanning calorimetry (DSC) measurements were used to characterize the change in the thermal properties of the polymers at a heating rate of 10 °C/min with a NETZSCH STA 449C. The thermal stability of the polyimide was performed by TGA under a N_2 environment on a Mettler-Toledo TGA/DSC instrument at a heating rate of 10 °C/min.

Shape-Memory Characterization. A flat sheet was employed to show the shape-memory process of the shape-memory polyimide more directly. The sheet was rolled into an semicylinder on the surface of hot stage in the ambient, and the shape was fixed by removal from the hot stage. The shape recovery on the surface of hot stage was recorded by a digital video (Canon VIXIA HF R500).

Shape Fixity and Recovery Measurement. Shape-memory cycles to assess shape fixity and recovery are measured using the controlled force mode on a TA Instruments Q800. The procedure for the cyclic tensile tests includes the following steps: (a) heating a sample to T_g + 40 °C at 10 °C/min, (b) applying a force that would elongate the sample, (c) reducing the temperature to T_g − 120 °C at 10 °C/min, (d) force removal, and (e) heating at 10 °C/min to T_g + 40 °C. Once recovery of the sample reached a constant value, the cycle was repeated by applying the same force used in step b.

RESULTS AND DISCUSSION

Thermoplastic Shape-Memory Polyimide. The polyimide was prepared by thermal curing of PAA, and the structures of PAA and PI were characterized with FTIR. The FTIR spectra demonstrate the imidization of the shape-memory polyimide,[44] as shown in the Supporting Information (Figure S1). The shape-memory polyimide samples are semitransparent, and the molecular weight can be adjusted by changing molar ratio of ODA/6FDA. The thermoplastic shape-

DOI: 10.1021/acs.macromol.5b00654
Macromolecules XXXX, XXX, XXX−XXX

Table 1. Physical Properties of Thermoplastic Shape-Memory Polyimides[a]

ODA/6FDA	title	M_n[b]	M_w[b]	T_g[c]	E' at T_g − 20 °C[d,f]	E' at T_g + 20 °C[d,f]	T_d[c]	R_f[e]	R_r[e]
1.000	TP0	61.5	110.9	316	1152 ± 32	10.7 ± 0.4	519	97.2	96.1
0.9850	TP1	50.2	105.3	314	1198 ± 38	11.1 ± 0.3	522	97.0	96.0
0.9625	TP2	38.4	85.4	311	1238 ± 52	9.4 ± 0.5	515	97.3	96.3
0.9400	TP3	25.8	60.6	304	1319 ± 58	6.7 ± 0.3	510	97.1	95.3
0.9250	TP4	21.3	47.0	299	1209 ± 41	6.4 ± 0.2	510	97.2	95.1

[a]Lower M_n, no shape-memory properties [b]In kg/mol. [c]In °C. [d]In MPa. [e]In %. [f]Average values and standard deviations.

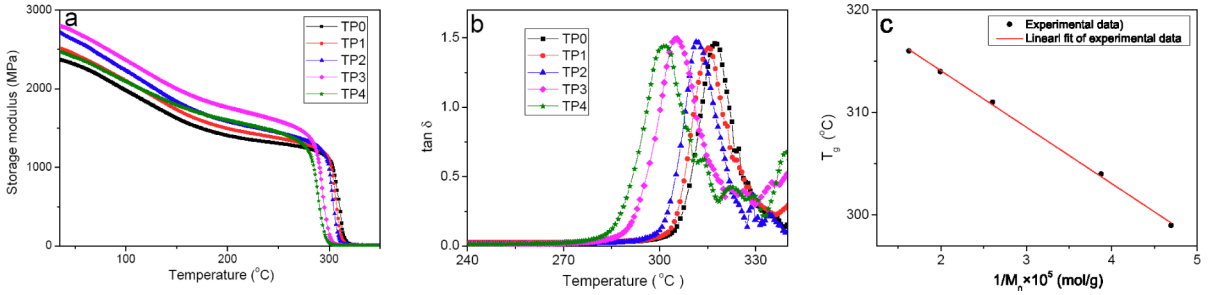

Figure 2. Thermomechanical properties of thermoplastic shape-memory polyimides: (a) tensile storage modulus, (b) loss factor, and (c) T_g versus reciprocal M_n of the polyimides.

memory polyimide samples with different M_n are labeled as TP0, TP1, TP2, TP3, and TP4, as indicated in Table 1.

TP0 with a stoichiometric ratio achieves the highest M_n of 61.5 kg/mol, while the stoichiometric imbalances cause a decrease in M_n, similar to other thermoplastic polyimides.[36] The critical molecular weight (M_c) is about 21.3 kg/mol, and samples with higher molecular weight ($M_n > M_c$) show the shape-memory effect, while samples with lower molecular weight ($M_n < M_c$) do not possess the shape-memory effect, similar to thermoplastic shape-memory polyurethanes.[41] For the polyimide with the molecular weight of M_n = 20.1 kg/mol (M_w = 43.8 kg/mol), although it can form a continuous film, it cannot fix the deformed shape very well. For the polyimide samples with the molecular weights of M_n = 17.1 kg/mol (M_w = 28.6 kg/mol) and M_n = 11.6 kg/mol (M_w = 26.9 kg/mol), they cannot form a continuous film but form the fragments. M_n exerts an influence on solubility, and although all polyimide samples can be dissolved in *N*-methylpyrrolidone (NMP), the samples with higher M_n are more difficult to be dissolved. TP0 and TP1 cannot be dissolved in dimethylformamide (DMF) while other samples can, and none of the samples can be dissolved in tetrahydrofuran (THF) or chloroform.

The thermomechanical properties of the samples are analyzed with DMA, and the tensile storage modulus (E') of the thermoplastic shape-memory polyimide samples versus temperature are shown in Figure 2a. It is seen that E' decreases slowly with the increase of temperatures in the glassy state, but there is a sharp drops of magnitude in the vicinity of softening point of the polyimide. For TP0, E' at 50, 260, and 340 °C are 2.3 GPa, 1.3 GPa, and 10.1 MPa, respectively. The large difference of E' in different states is necessary for the polymer to exhibit shape-memory effects. As the temperature gets higher, there is a plateau in the rubbery state, and the shapes of the elastic plateau are similar to each other, implying that the physical cross-links are mainly formed by chain entanglements.[7] It is observed that there is not a strong dependence of E' on molecular weight in glassy state, similar to that of the previously reported thermoplastic polyimide.[36]

Compared with differential scanning calorimetry (DSC), DMA is an effective and sensitive method to determine T_g of polymers with rigid molecular chains; here T_g of the shape-memory polyimide sample is obtained with DMA, and the DSC curve is shown in the Supporting Information (Figure S2). The loss factor (tan δ) versus temperature of the shape-memory polyimide samples is shown in Figure 2b. There is a clear tendency that T_g increases with the increase of M_n, as TP0 with the highest M_n show T_g of 316 °C and TP4 with the lowest M_n show T_g of 299 °C. The higher T_g of samples with higher M_n is associated with a greater degree of chain entanglement and higher intermolecular charge transfer complex interactions.[33]The relationship between T_g and M_n of the shape-memory polyimide is correlated with eq 1, namely a Fox−Flory equation.

$$T_g = T_{g\infty} - \frac{k_g}{M_n} \quad (1)$$

Here $T_{g\infty}$ is T_g of the sample with infinite molecular weight, and k_g is the parameter explaining the molecular weight dependence of T_g for the given material.[45] Figure 2c shows the experimental data and their linear fit according to eq 1. It is observed that the experimental T_g data are consistent with the predicted ones, exhibiting an adjusted *R*-square of 0.998. The extrapolation shows that the polyimide with infinite molecular weight would have a delineated T_g of 325.1 °C and k_g of -5.5×10^5 K mol g^{-1}.

The thermal stability of the thermoplastic shape-memory polyimides are examined with thermal gravimetric analysis (TGA), and the weight loss are shown in Figure 3. The weight loss of 5% is taken as the effective decomposition temperature (T_d), and T_d of the samples are listed in Table 1. It can be seen that T_d of all the samples are higher than 510 °C, and the pyrolysis left more than 50% carbonaceous char from the aromatic group at 700 °C for each sample, which means that the shape-memory polyimide samples are highly thermally stable. With the increase of temperatures, the weight of the polyimide gets less and less, and the carbonaceous char is more

DOI: 10.1021/acs.macromol.5b00654
Macromolecules XXXX, XXX, XXX−XXX

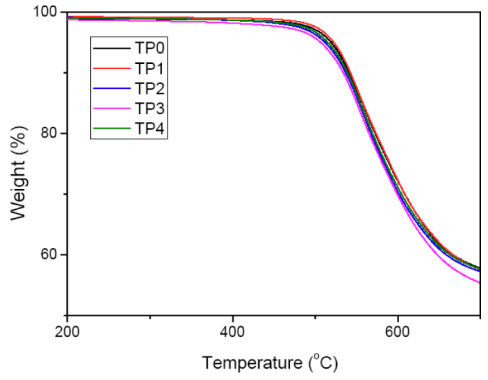

Figure 3. TGA spectra of thermoplastic shape-memory polyimides.

than 47% at 900 °C, as shown in the Supporting Information (Figure S3).

Shape recovery (R_r) is the ability of the material to recover to its original shape, and shape fixity (R_f) is the ability of the switching segments to hold the applied mechanical deformation during this process; they are two important factors in determining the-shape-memory effects of SMP. R_r is calculated using eq 2.

$$R_r(N) = \frac{\varepsilon_m(N) - \varepsilon_p(N)}{\varepsilon_m(N) - \varepsilon_p(N-1)} \times 100\% \quad (2)$$

Here ε_m , ε_p, and N denote the strain after the stretching step (before cooling), the strain after recovery, and the cycle number, respectively. R_f is calculated using eq 3.

$$R_f(N) = \frac{\varepsilon_u(N)}{\varepsilon_m(N)} \times 100\% \quad (3)$$

where ε_u denotes the strain in the fixed temporary shape. R_r and R_f are characterized with consecutive shape-memory cycles, and the cycles of TP0 are shown in Figure 4.

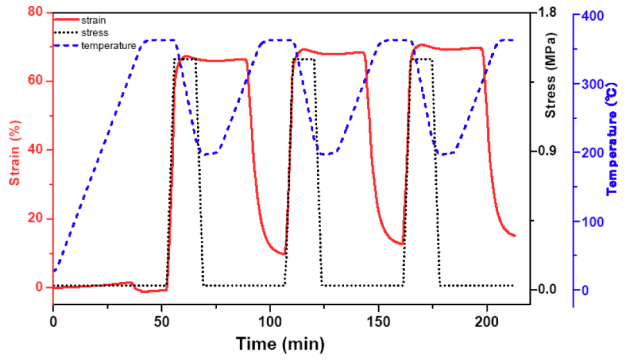

Figure 4. Consecutive shape-memory process of thermoplastic polyimide. The changes in strain, stress, and temperature in stress-controlled tensile process of TP0 are demonstrated.

It is observed that R_f are 97.1%, 97.2%, and 97.1%, respectively, which are consistent from one cycle to another. R_r was 85.6% for the first cycle and 96.1% and 96.6% for the second and third cycles. The difference in R_r between the first and the following cycles is generally attributed to residual strain resulting from the processing history of the sample.[46] As the reproducibility of R_f and R_r for each sample is good, the values of the second cycle are employed as the shape-memory parameters for the samples, and they are summarized in Table 1. It is observed that all the sample possess R_f higher than 97%, and R_r ranges from 96.1% to 91.1%, with TP4 with lowest M_n showing the lowest R_r. The high R_f and R_r of the thermoplastic shape-memory polyimide mainly originate from the high modulus below T_g and excellent rubber elasticity above T_g, which cause a sharp decrease in storage modulus from glassy to rubbery state. The high storage modulus is due to the potential elasticity in glassy state, and the low value is due to the entropy elasticity caused by the micro-Brownian movement in rubbery state. The well-defined rubbery plateau is important in the recycle thermal processing of the material, where stable thermal mechanical properties are required.

Thermoset Shape-Memory Polyimides. Thermoset SMPs are expected to find applications in many harsh environments, and tris(4-aminophenyl)amine (TAP) with three amine functional groups is employed as cross-link agent to form thermoset shape-memory polyimides. Thermoset polymer usually possesses higher T_g than the corresponding thermoplastic polymer, and the increase of T_g for thermoset shape-memory polyimide results from both disappearance of chain ends and formation of chemical cross-links. The effective cross-link density that causes the change can be calculated with the DiMarzio equation

$$\frac{T_{(x)} - T_{(0)}}{T_{(0)}} = \frac{KMX/\gamma}{1 - KMX/\gamma} \quad (4)$$

where $T_{(x)}$ is T_g of the covalent cross-linked polyimide, $T_{(0)}$ is T_g of the corresponding thermoplastic counterparts, K is often taken as 1.3×10^{-23}, M is the molecular weight of the imides repeat unit, X is the effective cross-link density, and γ is the number of flexible bonds per repeat unit.[47] The thermoset shape-memory polyimide samples with different TAP content are labeled as TS1, TS2, TS3, and TS4, as manifested in Table 2.

It is observed that while the thermoplastic shape-memory polyimides can be dissolved in NMP, the TAP covalent cross-linked shape-memory polyimide swelled in NMP, indicating that cross-linking has taken place. The swelling tests were conducted, and the results are shown in the Supporting Information (Table S1). The gel content increases with the increase of cross-linker and levels off when the cross-linker is 4%, from 35.6% for TS1 to 98.2% for TS3. The swelling ratio decreases from 17.3 for TS1 to 1.96 to TS4. These results show

Table 2. Physical Properties of Thermoset Shape-Memory Polyimides

TAP[a]	title	T_g[b]	ΔT[b]	DiMarzio X[c]	E' at $T_g - 20$ °C[d,e]	E' at $T_g + 20$ °C[d,e]	T_d[b]	R_f[a]	R[a]
1	TS1	322	8	2.83×10^{19}	1326 ± 75	13.0 ± 0.3	519	98.8	98.1
2.5	TS2	323	13	4.58×10^{19}	1210 ± 47	12.9 ± 0.2	520	98.6	98.5
4	TS3	322	17	6.01×10^{19}	1305 ± 62	13.6 ± 0.5	517	99.2	98.8
5	TS4	321	21	7.45×10^{19}	1225 ± 50	17.8 ± 0.6	518	98.5	98.9

[a]In %. [b]In °C. [c]In g^{-1}. [d]In MPa. [e]Average values and standard deviations.

DOI: 10.1021/acs.macromol.5b00654
Macromolecules XXXX, XXX, XXX−XXX

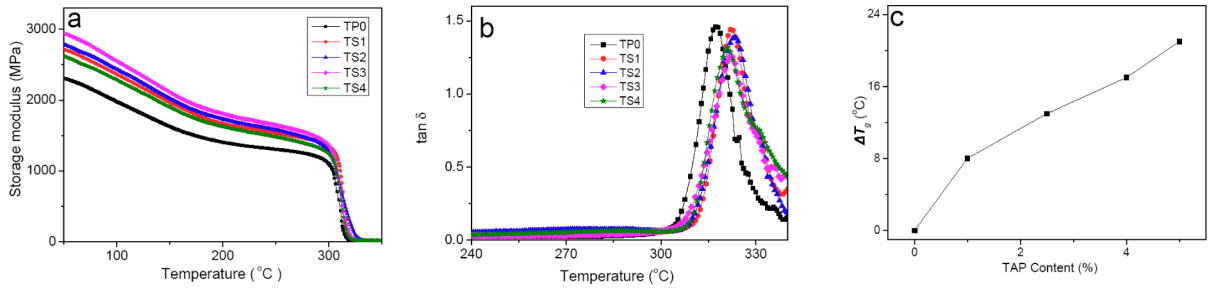

Figure 5. Thermomechanical properties of thermoset shape-memory polyimides with TP0 as reference: (a) tensile storage modulus, (b) tan δ versus temperature, and (c) difference in T_g (ΔT_g) between thermoset polyimide and thermoplastic counterpart.

that more TAP lead to higher chemical cross-link densities and result in a decrease in swelling by volume percentage.[48]

E' of the thermoset shape-memory polyimides are characterized with DMA, and the results are shown in Figure 5a with TP0 as reference. E' of thermoset polyimide sample at 50 °C is higher than 2.6 GPa, which indicates that covalent cross-linking can affect the mechanical properties of the samples. There is not a linear relationship between the content of TAP and E' in glassy state, similar to that of aspartimide-based SMPs.[34] However, E' in the rubbery plateau at high temperatures increases with the increase of cross-link density, ranging from 13 to 18 MPa. E' of the thermoset shape memory polyimides in the range of 325−345 °C are shown in the Supporting Information (Figure S4). An important practical point for applications is that E' of the thermoset polyimides in the rubbery state are relatively high for an unreinforced polymer, which is a desirable feature for a shape-memory polymer as it will give rise to a relatively high restoring force if recovery is resisted.

The loss factor of the shape-memory polyimide is shown in Figure 5b, and it can be seen that although the thermoplastic TP0 and thermoset polyimides possess stoichiometric ratio of anhydride to amine, T_g of TP0 is lower than others. Unlike thermoplastic polyimides, T_g of thermoset polyimides varies in a small range of 321−323 °C. Thermoset samples show higher T_g than their thermoplastic counterparts, and the difference between their T_g (ΔT_g) becomes larger with the increase of TAP content, from 8 °C for TS1 to 21 °C for TS4, as manifested in Figure 5c. The calculated cross-link density using DiMarzio's theory increases with the increase of cross-linker content and ranges from 2.83 × 10^{19} to 7.45 × 10^{19} g^{-1}, as summarized in Table 2.

It has been proved that for the cross-linker molecules with multiple functional groups not all the functional groups are covalently connected with polymer chains due to the space hindrance and reaction activity.[49] It is obvious that neither the cross-link density nor the M_n value is proportional to TAP content, which suggested that TAP acts not only as cross-linkers but also as chain extenders, similar to other covalent cross-linked systems reported.[50] The schematic illustration for the structure of thermoset shape-memory polyimides is manifested as Figure 6.

The thermal stability of the thermoset shape-memory polyimide is studied with TGA, and the weight loss versus temperature is shown in Figure 7. T_d of the thermoset samples are in the range of 517−520 °C, and the pyrolysis left more than 50% carbonaceous char from the aromatic group at 700 °C for each sample, which means that the thermoset shape-memory polymers are highly thermally stable.

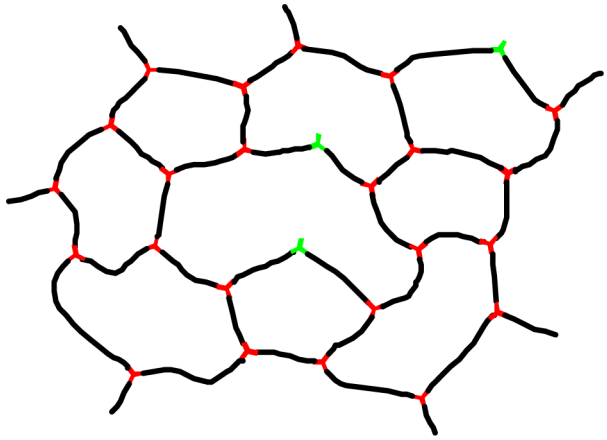

Figure 6. Schematic illustration of thermoset shape-memory polyimide. The black lines represents the polyimide chains; the red and green Y-type symbols represents TAP acting as cross-linkers and chain extenders, respectively.

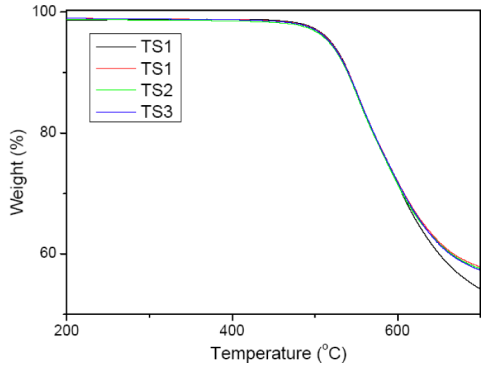

Figure 7. TGA spectra of thermoset shape-memory polyimide samples.

The shape-memory properties of the thermoset polyimide are studied with the same procedures of the thermoplastic polyimide, and all the thermoset shape-memory polyimdes show excellent shape-memory performances with R_r higher than 98% and R_f nearly 99%; the detailed data are shown in Table 2. The shape-memory process is more directly manifested when the sample is deformed into a semicylinder shape on a T_g + 40 °C hot stage, and the contemporary shape is fixed by removing the sample from the hot stage to room temperature. Upon reheating on the same hot stage, the material returns to the original form. The typical images showing the shape recovery process of TS3 are shown in Figure 8, and the movie is in the Supporting Information (Movie S1).

DOI: 10.1021/acs.macromol.5b00654
Macromolecules XXXX, XXX, XXX−XXX

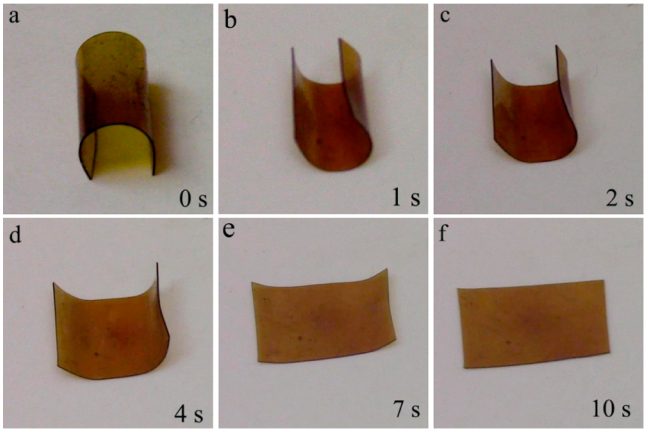

Figure 8. Shape recovery process of thermoset shape-memory polyimide: (a) the deformed shape and (b–f) the shape recovery process of TS3 on 360 °C hot stage. The subscripts indicate the time on the hot stage.

The process is repeated ten times with no damage observed, and every time the sample appears to recover fully to the initial shape. The consecutive shape-memory cycles of TS3 are shown in the Supporting Information (Figure S5), and other deformation modes like bending also show similar results.

Mechanism of the Shape-Memory Effects of Polyimide. The shape-memory effect of SMP is generally explained by dual-state mechanism, in which the molecular chains are regarded as the reversible phase and the nodes of macromolecule segments attributed to physical or chemical cross-links are regarded as the permanent phase.[1,5,43] It is observed that for the thermoplastic shape-memory polyimides the samples with M_n lower than 21.3 kg/mol do not possess shape-memory effects, which demonstrates that the permanent phase is mainly determined by chain entanglement of the polyimides with long chains. TAP acts as cross-linker and chain extender to form thermoset shape-memory polyimides, where the chemical covalent cross-links create a network topology on the molecular scale analogous to that created by physical entanglement on the mesoscale.[7] The shape-memory behavior of thermoplastic and thermoset polyimides are schematically illustrated in Figure 9, where R_f is 100% if $\Delta L = \Delta L'$ and R_r is 100% if $L_0 = L_0'$. The thermoset shape-memory polyimides exhibit better shape-memory performances than thermoplastic counterparts, mainly due to the loss in physical cross-link integrity of thermoplastic polyimide caused by mechanical deformation.[7]

The present common SMPs with low to medium shape transition temperature (T_g <110 °C) are mainly composed of polymers with flexible main chains, while SMPs with high T_g such as polyaspartimide, polyimide, cayanate, and PEEK ionomers are all characteristic of the rigid chains comprising phenyl rings and flexible linkages.[7,26−31] The shape-memory polyimide samples are obtained from polycondensation of dianhydride and diamine, and the polyimide in the current research is obtained by polycondensation of 6FDA/ODA. The hexafluoroisopropylidene and ether linkage within the backbone provide some flexibility to the highly aromatic polyimide structures, and the molecular chains act as reversible phase. With stoichiometric ratio of dianhydride and diamine, the shape-memory polyimide based on 4,4′-oxydiphthalic dianhydride (ODPA)/ODA, 6FDA/1,3-bis(3-aminophenoxy)benzene (BAB), and bis phenol A dianhydride (BPADA)/2,2-bis[4-4(-aminophenoxy)phenyl]propane (BAPP) exhibited T_g of 260.7, 222, and 212 °C, respectively.[13,27,28] The chemical structures of the above-mentioned shape memory polyimide samples are illustrated in the Supporting Information (Figure 6S). For dianhydrides, ODPA possess one ether linkage and BPADA possesses one isopropylidene and two ether linkages, while 6FDA possesses one hexafluoroisopropylidene in the backbone. For diamines, BAPP possesses an isopropylidene and two ether linkages, BAB possesses two ether linkages, and ODA possesses one ether linkage in the backbone. It is observed from their chemical structures that there is an obvious increase of flexibility of the polyimide chains, following the sequence of BPADA/BAPP > 6FDA/BAB > ODPA/ODA > 6FDA/ODA. The relative flexibility of the polymer backbone can affect dynamics through the glass transition,[42] and the polyimide of 6FDA/ODA accordingly exhibits T_g higher than previously reported ones.

CONCLUSION

In summary, this research provides some SMPs candidates for high-temperature applications. The aromatic polyimide chains possessing thermal stable but flexible units within the backbone can act as the reversible phase for high-temperature shape-memory effect, and the relative flexibility has a great influence on T_g. High M_n is needed to form physical cross-link, and T_g can be adjusted from 299 °C to delineated 325.1 °C by controlling M_n of thermoplastic shape-memory polyimide. Thermoset shape-memory polyimide shows higher T_g and better shape-memory performances than the thermoplastic counterpart due to the low density covalent cross-linking. This paper has offered some useful approaches to obtain high-temperature SMPs with desired T_g and thermomechanical and

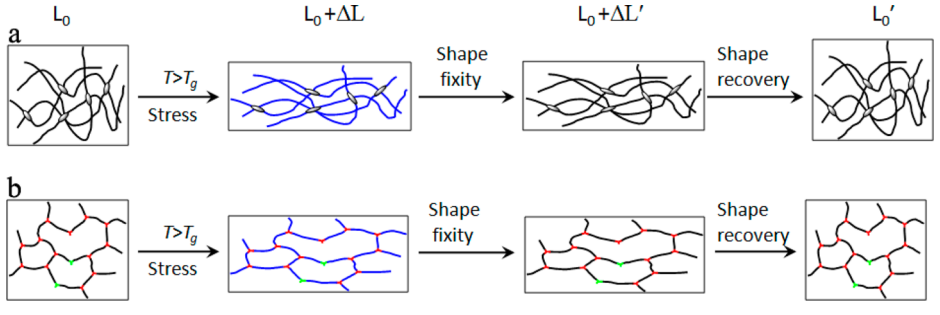

Figure 9. Schematics of shape-memory behavior of polyimides when T_g is used as shape recovery temperature: (a) thermoplastic polyimides where nodes are mainly chain entanglements; (b) thermoset polyimides where nodes are mainly covalent cross-links.

DOI: 10.1021/acs.macromol.5b00654
Macromolecules XXXX, XXX, XXX−XXX

shape-memory properties by tailoring chemical structure, molecular weight, and cross-link density. The mechanism of high-temperature shape-memory effects of polyimide is suggested, and further research on high-temperature shape-memory polymers will be stimulated.

■ ASSOCIATED CONTENT

Supporting Information

FTIR, DSC, and TGA spectra with the temperature to 900 °C for thermoplastic shape-memory polyimide; gel content, swelling ratio, tensile storage moduli from 325 to 345 °C, shape recovery process on the hot stage, and consecutive shape-memory process for thermoset shape-memory polyimides; molecular structures of the typical shape memory polyimides with different glass transition temperatures. The Supporting Information is available free of charge on the ACS Publications website at DOI: 10.1021/acs.macromol.5b00654.

■ AUTHOR INFORMATION

Corresponding Author

*E-mail: lengjs@hit.edu.cn (J.L.).

Author Contributions

X.X. conceived and designed the research, carried out most of experiments, analyzed the data and composed the manuscript. D.K., X.Q., and W.Z. performed the synthesis of shape-memory polyimides, molecular weight measurement, and shape-memory characterizations. L.L and Y.L. performed DMA and DSC characterization. S.Z. and H.Y performed IR and TGA characterization. J.L. offered advice on the design on shape-memory polyimide and oversaw the preparation of the manuscript. The manuscript was written through contributions of all authors. All authors have given approval to the final version of the manuscript.

Notes

The authors declare no competing financial interest.

■ ACKNOWLEDGMENTS

Dr. Tongxin Chang in Changchun Institute of Applied Chemistry is highly appreciated for her assistance in the measurements of molecular weight. This research is financially supported by National Natural Science Foundation of China (Grants 51402073, 11225211, and 11272106), China Postdoctoral Science Foundation (Grant 2013M531030), and Fundamental Research Funds for the Central Universities (Grant HIT. NSRIF. 2011018 and 2012064).

■ REFERENCES

(1) Tobushi, H.; Hara, H.; Yamada, E.; Hayashi, S. *Smart Mater. Struct.* **1996**, *5*, 483−491.
(2) Jeon, H. G.; Mather, P. T.; Haddad, T. S. *Polym. Int.* **2000**, *49*, 453−457.
(3) Behl, M.; Razzaq, M. Y.; Lendlein, A. *Adv. Mater.* **2010**, *22*, 3388−3410.
(4) Zhang, C. S.; Ni, Q. Q.; Fu, S. Y.; Kurashiki, K. *Compos. Sci. Technol.* **2007**, *67*, 2973−2980.
(5) Sokolowski, W. M.; Tan, S. C. *J. Spacecr. Rockets* **2007**, *44*, 750−754.
(6) Tandon, G.; Goecke, K.; Cable, K.; Baur, J. *J. Int. Mater. Syst. Struct.* **2009**, *20*, 2127−2143.
(7) Rousseau, I. A. *Polym. Eng. Sci.* **2008**, *48*, 2075−2089.
(8) Hu, J.; Zhu, Y.; Huang, H.; Lu, J. *Prog. Polym. Sci.* **2012**, *37*, 1720−1763.
(9) Khaldi, A.; Elliott, J. A.; Smoukov, S. K. *J. Mater. Chem. C* **2014**, *2*, 8029−8034.
(10) Scott, T. F.; Draughon, R. B.; Bowman, C. N. *Adv. Mater.* **2006**, *18*, 2128−2132.
(11) Yi, D. H.; Yoo, H. J.; Mahapatra, S. S.; Kim, Y. A.; Cho, J. W. *J. Colloid Interface Sci.* **2014**, *432*, 128−134.
(12) Schmidt, A. M. *Macromol. Rapid Commun.* **2006**, *27*, 1168−1172.
(13) Wang, Q. H.; Bai, Y. K.; Chen, Y.; Ju, J. P.; Zheng, F.; Wang, T. M. *J. Mater. Chem. A* **2015**, *3*, 352−359.
(14) Thomsen, D. L.; Keller, P.; Naciri, J.; Pink, R.; Jeon, H.; Shenoy, D.; Ratna, B. R. *Macromolecules* **2001**, *34*, 5868−5875.
(15) Kratz, K.; Madbouly, S. A.; Wagermaier, W.; Lendlein, A. *Adv. Mater.* **2011**, *23*, 4058−4062.
(16) Yakacki, C. M.; Shandas, R.; Lanning, C.; Rech, B.; Eckstein, A.; Gall, K. *Biomaterials* **2007**, *28*, 2255−2263.
(17) Lu, Y. C.; Fulcher, J. T.; Tandon, G. P.; Foster, D. C.; Baur, J. W. *Polym. Test.* **2011**, *30*, 563−570.
(18) Nagahama, K.; Ueda, Y.; Ouchi, T.; Ohya, Y. *Biomacromolecules* **2009**, *10*, 1789−1794.
(19) Chen, H.; Li, Y.; Liu, Y.; Gong, T.; Wang, L.; Zhou, S. *Polym. Chem.* **2014**, *5*, 5168−5174.
(20) Monkman, G. J. *Mechatronics* **2000**, *10*, 489−498.
(21) Haberl, J. M.; Sánchez-Ferrer, A.; Mihut, A. M.; Dietsch, H.; Hirt, A. M.; Mezzenga, R. *Adv. Funct. Mater.* **2014**, *24*, 3179−3186.
(22) Liu, Y. P.; Gall, K.; Dunn, M. L.; Greenberg, A. R.; Diani, J. *Int. J. Plast.* **2006**, *22*, 279−313.
(23) Liu, Y. J.; Du, H. Y.; Liu, L. W.; Leng, J. S. *Smart Mater. Struct.* **2014**, *23*, 023001.
(24) Paillous, A.; Pailler, C. *Composites* **1994**, *25*, 287−295.
(25) Wienhold, P. D.; Persons, D. F. *SAMPE J.* **2003**, *39*, 6−17.
(26) Shumaker, J. A.; McClung, A. J. W.; Baur, J. W. *Polymer* **2012**, *53*, 4637−4642.
(27) Yoonessi, M.; Shi, Y.; Scheiman, D. A.; Lebron-Colon, M.; Tigelaar, D. M.; Weiss, R. A.; Meador, M. A. *ACS Nano* **2012**, *6*, 7644−7655.
(28) Koerner, H.; Strong, R. J.; Smith, M. L.; Wang, D. H.; Tan, L. S.; Lee, K. M.; White, T. J.; Vaia, R. A. *Polymer* **2013**, *54*, 391−402.
(29) Xie, F.; Huang, L. N.; Liu, Y. J.; Leng, J. S. *Polymer* **2014**, *55*, 5873−5879.
(30) Shi, Y.; Yoonessi, M.; Weiss, R. A. *Macromolecules* **2013**, *46*, 4160−4167.
(31) Shi, Y.; Weiss, R. A. *Macromolecules* **2014**, *47*, 1732−1740.
(32) Harris, F. W. *Polyimides*, 1st ed.; Wilson, D., Stenzenberger, H. D., Hergenrother. P. M., Eds.; Chapman and Hall: New York, 1990; Vol. *1*, pp 9−12.
(33) Park, C.; Smith, J. G.; Connell, J. W., Jr.; Lowther, S. E.; Working, D. C.; Siochi, E. J. *Polymer* **2005**, *46*, 9694−9701.
(34) Wu, S.; Hayakawa, T.; Kakimoto, M. A.; Oikawa, H. *Macromolecules* **2008**, *41*, 3481−3487.
(35) Lebron-Colon, M.; Meador, M. A.; Gaier, J. R.; Sola, F.; Scheiman, D. A.; McCorkle, L. S. *ACS Appl. Mater. Interfaces* **2010**, *2*, 669−676.
(36) Hou, T. H.; Bryant, R. G. *High Perform. Polym.* **1997**, *9*, 437−448.
(37) Wang, D. H.; Arlen, M. J.; Baek, J. B.; Vaia, R. A.; Tan, L. S. *Macromolecules* **2007**, *40*, 6100−6111.
(38) Liaw, D. J.; Wang, K. L.; Huang, Y. C.; Lee, K. R.; Lai, J. Y.; Ha, C. S. *Prog. Polym. Sci.* **2012**, *37*, 907−974.
(39) Chen, S. J.; Hu, J. L.; Liu, Y. Q.; Liem, H. M.; Zhu, Y.; Meng, Q. H. *Polym. Int.* **2007**, *56*, 1128−1134.
(40) Nicholson, L. M.; Whitley, K. S.; Gates, T. S. *Int. J. Fatigue* **2002**, *24*, 185−195.
(41) Merline, J. D.; Reghunadhan, N. C. P.; Gouri, C.; Bandyopadhyay, G. G.; Ninan, K. N. *J. Appl. Polym. Sci.* **2008**, *107*, 4082−4092.
(42) Xie, T.; Rousseau, I. A. *Polymer* **2009**, *50*, 1852−1856.
(43) Warren, P. D.; McGrath, D. V.; Geest, J. P. V. *Mater. Eng.* **2010**, *295*, 386−396.
(44) Pryde, C. A. *J. Polym. Sci., Part A: Polym. Chem.* **1989**, *27*, 711−724.

DOI: 10.1021/acs.macromol.5b00654
Macromolecules XXXX, XXX, XXX−XXX

(45) Fox, J. T. G.; Flory, P. J. *J. Appl. Phys.* **1950**, *21*, 581−591.
(46) Chung, T.; Rorno-Uribe, A.; Mather, P. T. *Macromolecules* **2008**, *41*, 184−192.
(47) Kelch, S.; Choi, N. Y.; Wang, Z. G.; Lendlein, A. *Adv. Eng. Mater.* **2008**, *10*, 494−502.
(48) Di Marzio, E. A. *J. Res. Natl. Inst. Stand. Technol.* **1964**, *6*, 611−617.
(49) Miller, D. R.; Macosko, C. W. *Macromolecules* **1976**, *9*, 199−206.
(50) Buckley, C. P.; Prisacariu, C.; Caraculacu, A. *Polymer* **2007**, *48*, 1388−1396.

DOI: 10.1021/acs.macromol.5b00654
Macromolecules XXXX, XXX, XXX−XXX